Materials and Design 201 (2021) 109454

Contents lists available at ScienceDirect

Materials and Design

journal homepage: www.elsevier.com/locate/matdes

Downshifting and antireflective thin films for solar module power enhancement

Yujuan He [a], Jie Liu [b], Shi-Joon Sung [c], Chih-hung Chang [a,*]

[a] School of Chemical, Biological & Environmental Engineering, Oregon State University, Corvallis, OR 97331, United States
[b] College of Physical Science and Technology, Dalian University, Dalian, Liaoning 116622, China
[c] Convergence Research Center for Solar Energy, DGIST, Daegu 42988, Republic of Korea

HIGHLIGHTS

- Graded thin films are designed to enhance UV and visible photon utilization.
- The graded thin films increase the PCE of the pc-Si solar cell by 4.12%.
- The optical properties of graded thin films are simulated by the FDTD method.

GRAPHICAL ABSTRACT

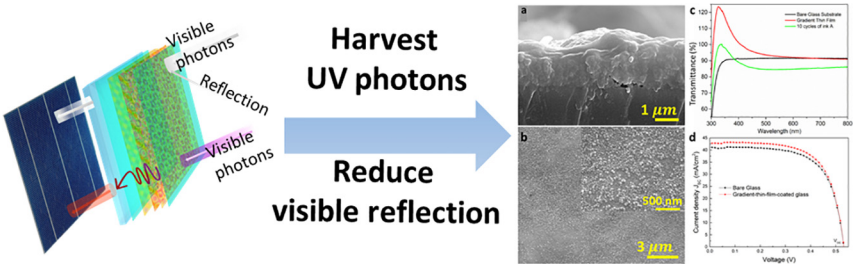

ARTICLE INFO

Article history:
Received 25 August 2020
Received in revised form 5 January 2021
Accepted 6 January 2021
Available online 12 January 2021

Keywords:
Downshifting
Antireflection
Graded multifunctional thin film
Finite difference time domain (FDTD)
Si solar cell

ABSTRACT

Efforts to enhance the solar conversion efficiency have prevailed for decades. There is a growing interest in improving the spectral response of solar modules, especially in harvesting UV photons, which offer intense energy in a narrow wavelength range. To harvest UV photons and reduce reflection without interfering with the formulas and manufacturing process of solar cells, in this work, thin films that possess downshifting and antireflection capabilities were fabricated on the cover glass of multicrystalline Si solar cells. The thin films were composed of graded index layers of europium-doped yttrium orthovanadate (YVO_4:Eu) and hollow silica nanoparticles (HSNPs). The design of the composite thin films was assisted by the FDTD mathematical model that simulated the refractive index and thickness of each layer to obtain the optimum transmittance. The cover glass with multifunctional thin films harvested more than 30% of UV photons and enhanced the solar conversion efficiency by 4.12% at normal incidence compared to the uncoated cover glass.

1. Introduction

The maximum efficiency of a single-junction solar cell is bounded by the Shockley-Queisser limit. The majority of solar modules deployed in the field for terrestrial applications, including multicrystalline Si, crystalline Si, cadmium telluride (CdTe) and copper indium gallium (di)selenide (CIGS) thin film solar cells, are single-junction solar cells. These modules show inadequate spectral response to ultraviolet (UV) photons, which results in a significant portion of incident UV photons being absorbed in high recombination regions and not converting to photocarriers. The photon energy in the UV range accounts for 4.62% of solar energy (AM 1.5G spectrum) [1]. Current commercial Si solar photovoltaic modules, including monocrystalline and multicrystalline Si, which have been widely used in the field and account for more than 90% of total solar photovoltaic production, can achieve high photon conversion efficiency in the visible and near-infrared (NIR) regions but not in the UV region. Additionally, the unused UV photons can have negative impacts on the Si solar PV modules, such as optical losses due to EVA browning and delamination.

The solar conversion efficiency (SCE) of organic-inorganic hybrid perovskite solar cells has increased from 3.81% to 22.1% in less than ten years. Despite such impressive progress, several challenges prevent the commercialization of perovskite solar cells, such as the lack of UV

* Corresponding author.
E-mail address: chih-hung.chang@oregonstate.edu (C. Chang).

https://doi.org/10.1016/j.matdes.2021.109454

stability. Thus, it is highly beneficial to utilize UV photons to improve the solar conversion efficiency of solar PV modules. Multijunction photovoltaics (PVs) is an elegant and effective approach to capture UV photons by stacking several PV materials with different optical bandgaps into one solar cell. Multijunction solar PVs can achieve the highest solar conversion efficiency with broad-spectrum coverage [2]; however, their high cost and convoluted fabrication processes are problematic for large-scale manufacturing.

Downshifting (DS) materials, which can convert higher-energy photons (e.g., UV photons) into lower-energy photons (e.g., NIR photons), were first proposed by Hovel et al. [3] to improve the spectral response of solar cells. The majority of these previous studies focused on integrating the downshifting materials directly on top of the solar cells or between the solar cell and the cover glass. For example, Klampaftis et al. incorporated multiple fluorescent dyes into the ethylene vinyl acetate (EVA) encapsulation layer of the polycrystalline silicon (pc-Si) solar cell and Cu(*In*, *Ga*)Se_2 (CIGS) solar cell, which resulted in a 0.18% higher absolute efficiency and a 1.8% higher short-circuit current density (JSC), respectively [4,5]. Alternatively, the DS materials can be incorporated with cover glass. This approach has three potential advantages: (1) there is no interference with the formulas and fabrication processes of solar cells; (2) it can be directly applied to the top of the cover glass of current solar modules in existing solar farms; and (3) more UV photons that are not reflected or absorbed by cover glass are available. T^{3+}-doped tellurite glass [6] and Tb^{3+}-Eu^{3+}-doped barium borate glass [7] were reported to increase the relative SCE of a commercial silicon solar cell by 7% and a CdTe solar cell by 1%, respectively. However, technical challenges still exist in manufacturing such glass on a large scale and in replacing the current cover glass. An effort to apply Eu^{3+}-doped PMMA film on top of cover glass was made to improve the response to UV photons [8]. One fundamental challenge of applying downshifting materials onto cover glass is maintaining and improving the transmittance of the cover glass in the visible or NIR regions. Merely applying phosphors on cover glass usually results in the reduction of the transmittance in the visible range since the phosphor refractive index (RI) is substantially discrepant from that of cover glass. In this study, we introduce hollow silica nanoparticles (HSNPs), which have a low RI, into a downshifting thin film to reduce the RI discrepancy. The composite thin film is assembled as graded index layers to avoid dilution of the DS material. The graded index layer can also further reduce the reflections, as reported in previous studies [9,10].

The commonly used DS phosphors include lanthanide phosphors, dyes, and quantum dots. Silicon quantum dots [11] and dyes have been reported to increase the SCE of solar cells by 4% and 17%, respectively [12,13]. Compared to dyes and quantum dots, lanthanide crystals have broad absorption in the UV region and adequate separation between absorption and emission peaks, which efficiently avoids self-absorption. Prior articles demonstrated that the absorption bandwidth of Si solar cells was broadened by lanthanide phosphors such as Y_2O_3:Eu [14], Ba_2SiO_4:Eu [15], and YVO_4:Bi, Ln [16]. The lanthanide luminescent crystals also possess excellent thermal, mechanical, and optical properties [17], which are critical when applying them to cover glass and under exposure to harsh environments. Europium-doped yttrium orthovanadate (YVO_4:Eu), one of the lanthanide luminescent crystals, is selected in this study due to its photostability, efficient quantum conversion, and broad absorption in the UV region (250–400 nm). The host crystal, YVO_4, has a relatively low RI of 2.0 and a high optical bandgap of 3.5 eV compared to other hosts such as titanium dioxide [18]. These properties allow the YVO_4 thin film on the cover glass to have a relatively high transmittance in the visible region according to the Fresnel equation [19]. YVO_4:Eu with different configurations has been used as a DS phosphor in various types of solar cells [20–22]. However, the optical performance when using YVO_4:Eu layers on cover glass has not been reported in the literature.

In this study, a composite thin film on cover glass (Fig. 1b & c) was designed to improve the response of multicrystalline Si solar cells in the UV region via wavelength downshifting and to enhance the transmission of visible photons by RI engineering. The thin film composed of the graded index layers was optically simulated by the finite difference time domain (FDTD) method to achieve an optimum transmittance in the range of 400–800 nm. The thin films fabricated according to the optimized parameters possessed both downshifting and antireflection capabilities.

2. Methods and materials

2.1. FDTD model

The thin film of five graded index layers on a glass substrate was optically simulated by the finite-difference time-domain (FDTD) model of Lumerical FDTD Solution 8.19.1416. Two-dimensional (2D) Maxwell's equations were used in our model. Each layer of the graded thin film (Fig. 1) was modeled as a bulk material, for which the thickness and refractive index were defined or set as parameters to be optimized. A plane wave imitated solar energy and provided laterally uniform electromagnetic energy to the top of the graded thin film. Two frequency domain power monitors (FDPMs) were used to record reflection and transmission. The total transmittance of the incident light through the graded film ($T_{sum} = 1 - R_{sum}$) was used as the criterion for the optimization of the RI and thickness of each layer. R_{sum} can be obtained by Eq. S3 in the supplementary material. More details of the FDTD model can be found in the supplementary material.

2.2. Multilayer film fabrication

Inks containing YVO_4:Eu and HSNPs (Table 1) were used to experimentally fabricate the multilayer thin film with optimized FDTD parameters. The inks were prepared by dispersing YVO_4:Eu powder and HSNP solution in ethanol via ultrasonication. A TEOS-based binder, which was an ethanol solution formulated with 1.26 M H_2O, 2.3 mM HCl, and 0.21 M TEOS, was added to the ink. The TEOS-based binder can affix the loose particles on the top of the substrate or the previous layer after baking at 60 $^{\circ}C$ for 30 min. The as-prepared inks (Table 1) were spin-coated onto a glass substrate of 1 cm × 1 cm at different revolutions per minute (rpm) to reach the optimized thickness proposed by the FDTD model. According to the calculated RI of each ink (Table 1) and the optimized parameters of the FDTD model (Table 2), the fabrication of the five-layer graded thin film was initiated by coating ink E onto a glass substrate, and then ink D, ink A, and ink C were sequentially applied. Finally, another layer of ink E was deposited on the top to complete the five-layer structure. The thickness of each layer, which was controlled by the coating cycles and rpm, was experimentally optimized to achieve the highest transmittance in the visible region. Each layer was cured at 60 $^{\circ}C$ for 30 min before applying the next layer. The TEOS-based binder and HSNP solution were added to the ink immediately before spin-coating. As shown in Table 1, the refractive index was controlled by the ratio between YVO_4:Eu and HSNPs according to the refractive index mixing rules (supplementary material, Eq. S1).

2.3. Materials and preparation

Tetraethyl orthosilicate (TEOS, reagent grade, MilliporeSigma), poly (acrylic acid) (PAA, MW = 5000, 50 wt% in aqueous solution, Polysciences), ammonium hydroxide (NH_4OH, 28–30%, MACRON), yttrium(III) nitrate hydrate ($Y(NO_3)_3.xH_2O$, 99.99%, Alfa Aesar), europium(III) nitrate hydrate ($Eu(NO_3)_3.xH_2O$, 99.99%, Alfa Aesar), sodium orthovanadate (Na_3VO_4, 99.98%, Alfa Aesar), sodium hydroxide (NaOH, pellets, >98%, ACS, MACRON), hydrochloride (HCl, MilliporeSigma) and ethanol (EtOH, ACS, MACRON) were used as received without any further purification. Deionized water (H_2O, 18 MΩ·cm, Millipore Milli-Q) was used throughout the experiment.

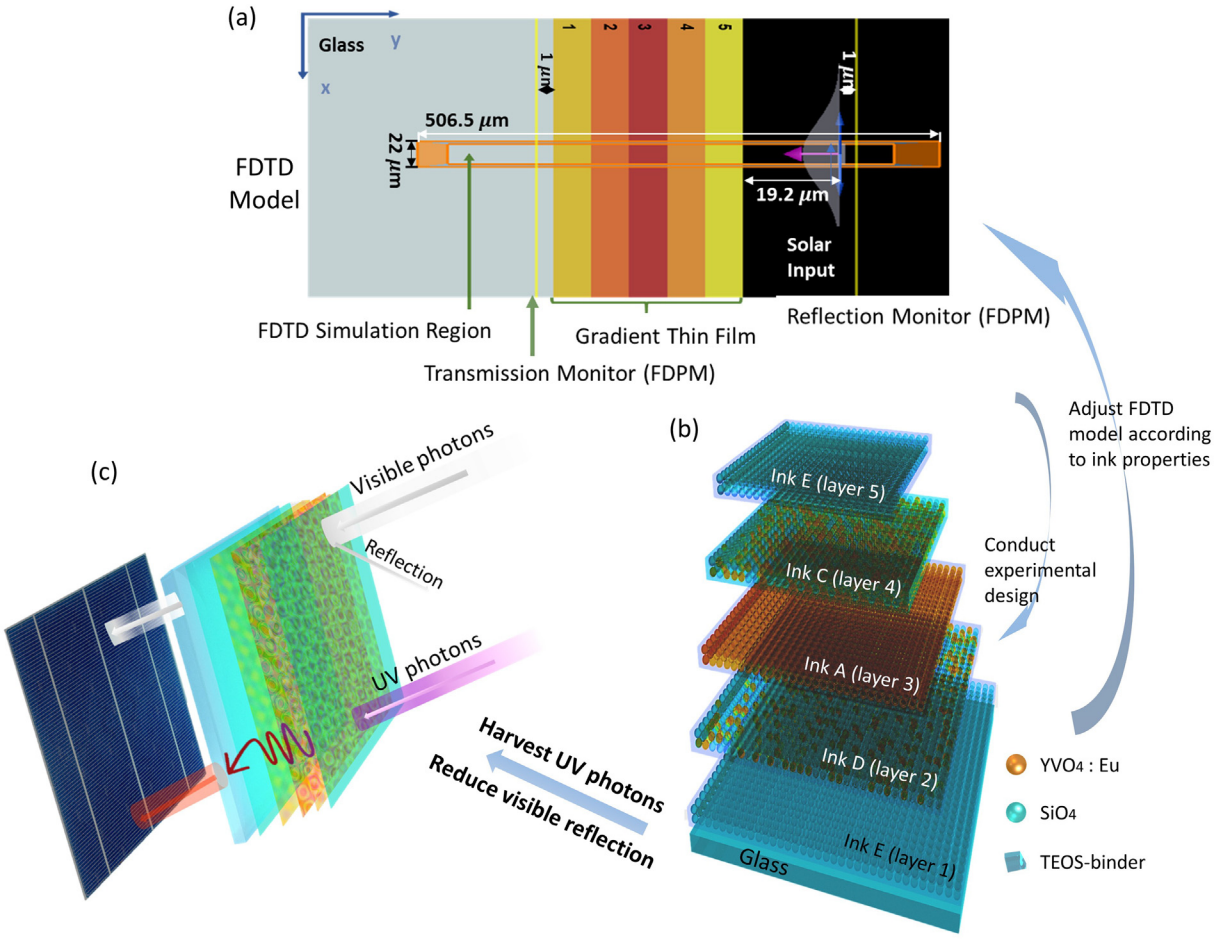

Fig. 1. (a) FDTD model and (b) schematic diagram of the graded thin film on cover glass. (c) Schematic diagram of the graded-thin-film-coated cover glass interacting with UV and visible photons.

Table 1
YVO_4: Eu and HSNP inks.

Ink	A	B	C	D	E
YVO_4:Eu (mg)	3.0	2.7	2.4	2.1	0
HSNPs vol. (μL)[1]	0	6.5	13	19.5	65.0
EtOH vol. (mL)	0.4	0.3994	0.3987	0.3981	0.3935
Refractive index	1.81	1.79	1.76	1.73	1.36

[1] 0.136 g HSNPs was redispersed in 10 mL EtOH.

Table 2
Optimized RI and thickness of each layer simulated by the FDTD method. (The user-defined figure of merit (FOM) history and trend of the simulation can be found in the supplementary material).

	Refractive index	Thickness
Layer 1	1.36	104
Layer 2	1.73	100
Layer 3	1.80	343
Layer 4	1.76	102
Layer 5	1.36	109

Hollow silica nanoparticles (HSNPs) were synthesized by the microfluidic-assisted method of He et al. [23]. The particle diameter of the HSNPs was 38.9 ± 9.7 nm. A TEM image of the HSNPs can be found in Fig. S1 (supplementary material). The HSNPs were washed with deionized water and ethanol. Finally, 0.136 g washed HSNPs was redispersed in 10 mL EtOH by ultrasonication. YVO_4:Eu nanoparticles were synthesized using the following hydrothermal batch reaction procedure: 3 at.% Eu^{3+} was doped in the YVO_4 crystal to obtain a maximum quantum yield and a comparatively long lifetime [24]. A 5 mL aqueous solution containing 0.11 M Na_3VO_4, 15 mM PAA and 0.14 M NaOH was added dropwise into another 5 mL aqueous solution with 3 mM $Eu(NO_3)_3$ and 100 mM $Y(NO_3)_3$ under continuous stirring at 600 RPM. The mixture was maintained at 200 °C for 24 h in a 50-mL autoclave (PPL high-temp polymer liner chamber, Col-Int Tech. LLC). The as-prepared YVO_4:Eu nanoparticles were washed with water and ethanol and then dried under vacuum at room temperature.

2.4. Characterization

An Ocean Optics USB2000 spectrograph fiber-coupled to an integrating sphere and a deuterium-halogen light source (DH-2000, Ocean Optics) was used to measure the absorbance in the range of 225–400 nm (supplementary material, Fig. S1). The absorption coefficient of YVO_4:Eu can be obtained by linearly fitting the absorbance at 275 nm for different concentrations based on the Beer-Lambert law (supplementary material). A UV–Vis-NIR spectrophotometer (Jasco V-670) was used to measure the transmittance of the coated samples. A spectrofluorometer (Horiba Jobin Yvon) was used to characterize the photoluminescence emission (PL) spectrum. Scanning electron microscopy (SEM, FEI Quanta 3D) was used to obtain top and cross-sectional views of the coated thin films. Transmission electron microscopy (TEM, FEI TITAN 80–200) was employed to provide an image of the as-synthesized

YVO_4:Eu. Selected area diffraction (SAED) was performed to identify the crystal phase of YVO_4:Eu. The solar conversion efficiency of the PV cells with coated and uncoated cover glass was measured by an Oriel 96,000 full spectrum solar simulator under AM 1.5G illumination.

3. Results and discussion

3.1. FDTD model of composite thin film

In the FDTD model of the single layer of YVO_4:Eu, the optimized thickness is obtained as 880 nm by sweeping the thickness from 50 nm to 1000 nm. Even with the optimized thickness, the maximum T_{sum} can only reach 93.9%, which is 5.04% lower than that of the simulated bare glass. The simulated spectrum in Fig. 2 indicates that the YVO_4:Eu transmittance over the entire wavelength is lower than that of the bare glass, which is consistent with the experimental data for above three cycles in Fig. 3e. In terms of film fabrication, films with thicknesses as high as 880 nm easily crack and have high scattering because of increased roughness. It is not practical to achieve adequate transmittance in the visible range by relying on a single layer of YVO_4:Eu. One feasible approach to increase the transmittance in the visible range for the downshifting film is to reduce its RI. HSNPs with a low RI of 1.12 [23] can be used to reduce the RI. However, adding HSNPs means reducing the amount of YVO_4:Eu in a single film and therefore diminishing the downshifting performance. Accordingly, a thin film of five graded index layers was applied to maintain the YVO_4:Eu content as well as the transmittance of the cover glass in the visible region. A schematic diagram of the graded film and its FDTD model is shown in Fig. 1. The optimized formulation (Table 2) reduces the average reflectance in the range of 450–850 nm by 30.6% and 14.3% relative to the simulated one-layer film and bare glass, respectively (Fig. 1). The mathematical simulation demonstrates the possibility of creating a downshifting film on a glass substrate without diminishing the transmittance in the visible region. The delicate adjustment of the RI by introducing more layers could further enhance the transmittance of the films. This study uses a five-layer thin film as a simple structure to demonstrate the proposed concept.

3.2. YVO_4: Eu layer

Before investigating the composite thin film, understanding the optical performance of YVO_4:Eu on a glass substrate is crucial. As presented in Fig. 3a & b, the transparent glass coated with the experimentally-prepared ink A emitted red light when illuminated by UV light at 254 nm. The amount of YVO_4:Eu on a substrate and the intensity of the emitted light increased with increasing spin-coating cycle from one to ten (Fig. 3e). The PL spectrum of the YVO_4:Eu-coated glass (10 cycles) in Fig. 3c presents the typical energy transitions $^5D_0 \rightarrow {}^7F_j$ (j = 1, 2, 3, 4) of europium. The main emission peak ($^5D_0 \rightarrow {}^7F_2$) and the secondary emission peak ($^5D_0 \rightarrow {}^7F_4$) are located at approximately 615 nm and 700 nm, respectively, where the pc-Si cell has high absorption [25]. YVO_4:Eu has a subwavelength size of 48.35 ± 14.22 nm, as shown in Fig. 3d. The SAED pattern (inset of Fig. 3d) indicates that YVO_4:Eu has the same (312), (200), and (112) crystal plane as the pure tetragonal (zircon) phase (JCPDS 72–0861) with unit cell parameters a = b = 7.123 Å and c = 6.292 Å.

The amount of YVO_4:Eu on glass substrates was experimentally quantified by its absorption coefficient. The absorption coefficient of the as-synthesized YVO_4:Eu was determined to be 1.213×10^3 $mmol^{-1}$ cm^2, based on Beer's law (supplementary material). The absolute absorbance of YVO_4:Eu coated on substrates (supplementary material, Fig. S4c) was determined by subtracting the reflection (supplementary material, Fig. S4b) from the measured absorbance (supplementary material, Fig. S4a) in the range of 225–400 nm. Combining the absolute absorbance spectrum with the absorption coefficient, the molar concentrations of YVO_4:Eu on glass substrates created by different coating cycles are shown in Fig. S4d in the supplementary material. More coating cycles result in more YVO_4:Eu deposited on substrates. The concentration of YVO_4:Eu on the substrate was increased by 76% from 4.25×10^{-4} mmol cm^{-2} to 7.5×10^{-4} mmol cm^{-2} (supplementary material, Fig. S4d). The typical sizes of residential and commercial solar modules are 1.64×10^4 cm^2 and 2.23×10^4 cm^2, respectively [26–28]. If the concentration of YVO_4:Eu is 7.5×10^{-4} mmol cm^{-2}, then 2.5 g and 3.4 g YVO_4:Eu are required to create a DS film on the cover glass of residential and commercial solar modules, respectively. The YVO_4:Eu used in this study contains 3 at.% europium, which provides relatively high quantum efficiency, as reported in previous research [24]. Approximately 0.54 g and 0.74 g europium precursor ($Eu(NO_3)_3$) are required to obtain 2.5 and 3.4 g YVO_4:Eu, respectively, as the synthesis yield is 30 wt%.

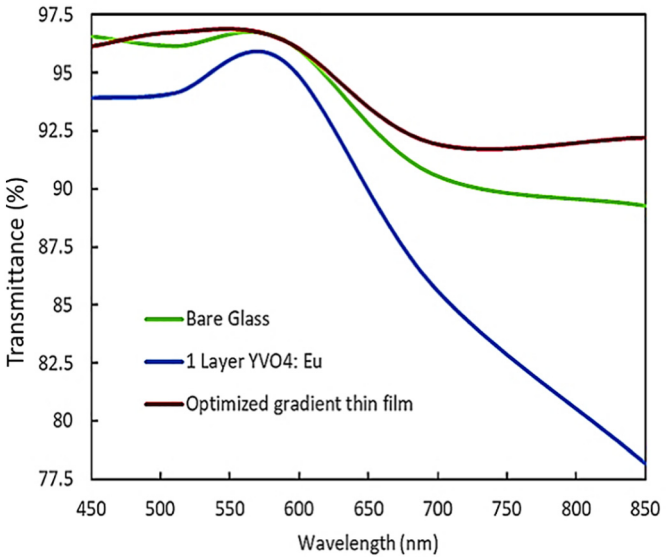

Fig. 2. Simulated transmittance spectra of bare glass with the one-layer YVO_4:Eu (ink A) coating and with the optimized graded-thin-film coating.

In addition to the optical performance in the UV region, the transmittance of the YVO_4:Eu-coated glass in the visible region (400–800 nm) is critical for its application to pc-Si solar modules. Accordingly, a JASCO UV–Vis-NIR spectrometer coupled to a 60-mm integrating sphere was used to measure the transmittance in the visible region. The integrating sphere enabled the collection of all transmitted and scattered photons. In the visible region, the glass substrates coated with ink A (YVO_4:Eu and TEOS-based binder) have a lower transmission than the bare glass (Fig. 3e). Depositing more YVO_4:Eu results in a significant decrease in the transmittance. Since both glass and YVO_4:Eu have low extinction coefficients and low absorption in the visible region, the transmittance decrease is mainly attributed to the reflectance generated by the light propagation in different media and can be described by the refractive index (RI). The Fresnel equation (Eq. (1)) can be used to determine the reflectance R of a thin-film-coated substrate at normal incidence, where n_{air}, n_s, and n are the RIs of air, the substrate, and the thin-film coated on the substrate, respectively [19]. The reflectance R achieves zero when n is equal to $\sqrt{n_{air}n_s}$, which is 1.23, where the substrate is glass with an n_s of 1.50 [29]. The film created from ink A is a composite of YVO_4:Eu and SiO_2 and has an RI of 1.81, which diverges from the ideal RI, resulting in strong reflections. The FDTD model of a single layer of YVO_4:Eu in Fig. 2 also shows that the YVO_4:Eu film on the glass substrate has higher reflectance than the bare glass.

$$R = \left[\frac{n_{air}n_s - n^2}{n_{air}n_s + n^2}\right]^2 \quad (1)$$

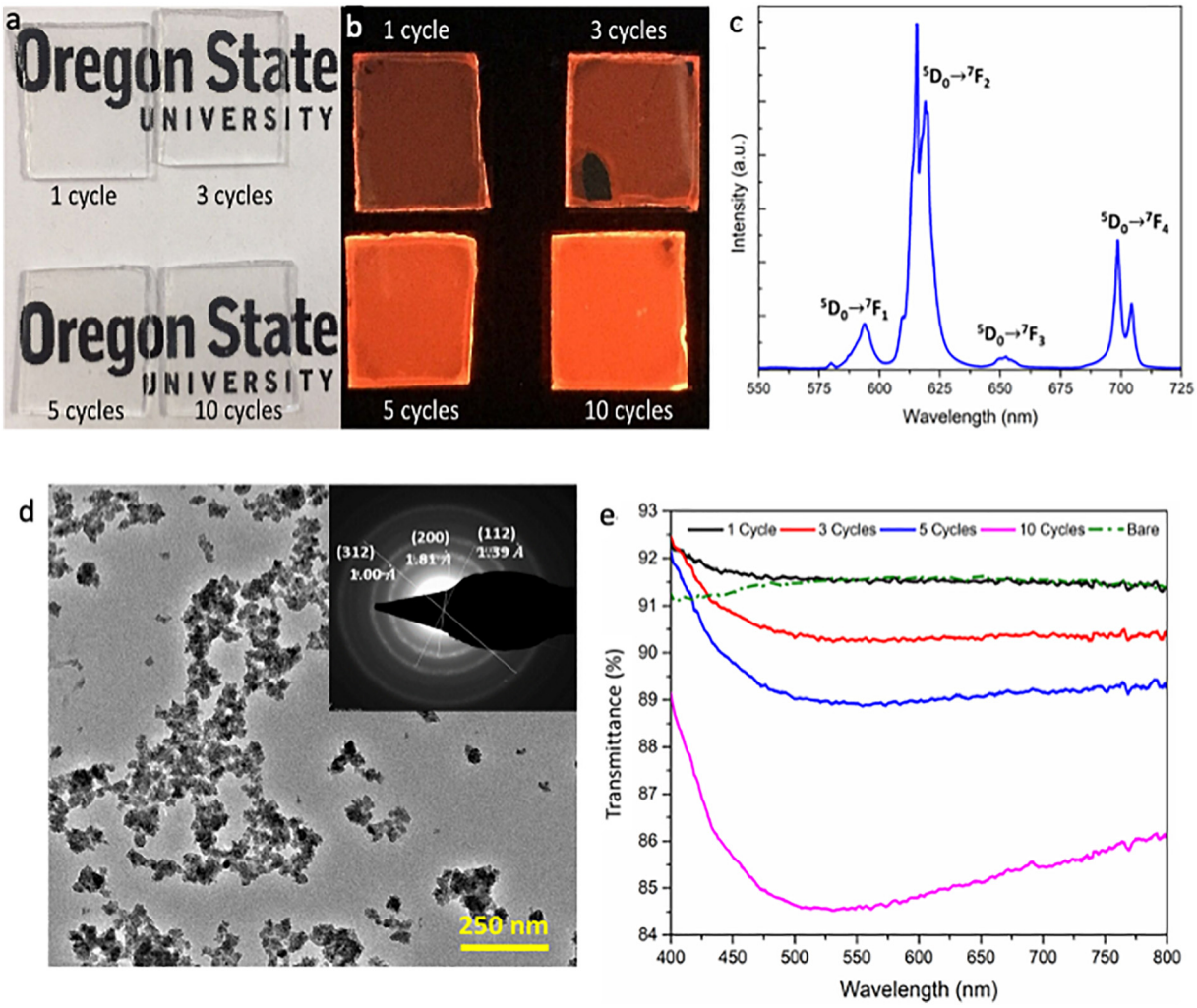

Fig. 3. (a) Optical images under normal daylight and (b) UV (254 nm) light of the YVO_4:Eu-coated glass substrates with different spin-coating cycles. (c) Photoluminescence emission spectrum of a YVO_4:Eu-coated glass substrate (10 cycles). (d) TEM image and SAED pattern (inset) of the as-synthesized YVO_4:Eu NPs. (e) Transmittance spectra of YVO_4:Eu-coated glass substrates.

3.3. Experimentally-fabricated composite thin film

According to the optimized RI of each layer in Table 2, inks of different RIs were experimentally formulated as shown in Table 1. Cross-sectional SEM images of the films made from inks A, B, C and D are presented in Fig. 4a–f. The film made from ink E primarily consists of dense silicon dioxide, which is hardly distinguishable from glass substrates. We found that increasing the mole ratio of HSNPs leads to a compact packing pattern and a reduction of the film thickness (volume), as shown in Fig. 4a–f. The HSNPs are well-defined spherical particles with a smaller diameter of approximately 30 nm [23] and an excellent dispersion in the TEOS-based binder compared to YVO_4:Eu. As described by the simulation model of Jia et al. [30], adding small particles can reduce the porosity and promote the coordination number of a thin film and therefore create a tight particle packing structure. The coordination number corresponds to the contact between a particle and its neighbors. A larger coordination number means more contact among particles and their neighbors. Additionally, HSNPs and YVO_4:Eu NPs interact differently with the glass substrate due to the difference in shape and surface structures. In our study, a higher volume ratio of HSNPs tends to provide a more uniform film and a better particle distribution on glass substrates (Fig. 4). Fig. 4g shows that the film of YVO_4:Eu is spotty and contains hills and valleys, which are formed by aggregated YVO_4:Eu. When the mole ratio of HSNPs is increased from zero to 10%, the hills and valleys are replaced by small islands (e.g., the bright sites circled in Fig. 4h). Due to the formation of islands, the cross-sectional views of ink B exhibit a discontinuous film where the thickness is hard to measure (supplementary material, Fig. S5). Ink B is inappropriate for creating a transparent film because its unevenly distributed islands are much larger than the visible wavelength. The film becomes increasingly smooth and dense when the mole ratio of HSNPs reaches 20% and 30% (Fig. 4i & j). The high-magnification images (insets of Fig. 4i & j) indicate that the particles are embedded in the films and form some small bulges. The bulges in the film of ink D are much smaller than those of ink C.

Fig. 5a & b shows the cross-sectional SEM view of the film of graded index layers. The layers likely intermix with each other. This intermixed structure might be due to the semihardened layer being redissolved by the freshly applied ink during spin-coating. The remixed particles likely settled and created an intermediate region between each layer. As discussed in previously published studies [31,32], the antireflective coating could benefit from the intermediate region which eliminates the rigid boundaries between two layers and consequently reduces the reflection created by the abrupt change in RI. The intermediate layer enabled the film to have a more delicate adjustment of the RI and therefore achieve a gradually varying RI in contrast to stacked multilayers. The top view of the graded thin film is presented in Fig. 5b, which shows a continuous film with some bulges. At high magnification (inset of Fig. 5b), well-defined spherical HSNPs assembled on the top can be observed.

The transmittance spectrum in Fig. 5c shows that the transmittance of the graded thin film is much higher in the visible region than that of the

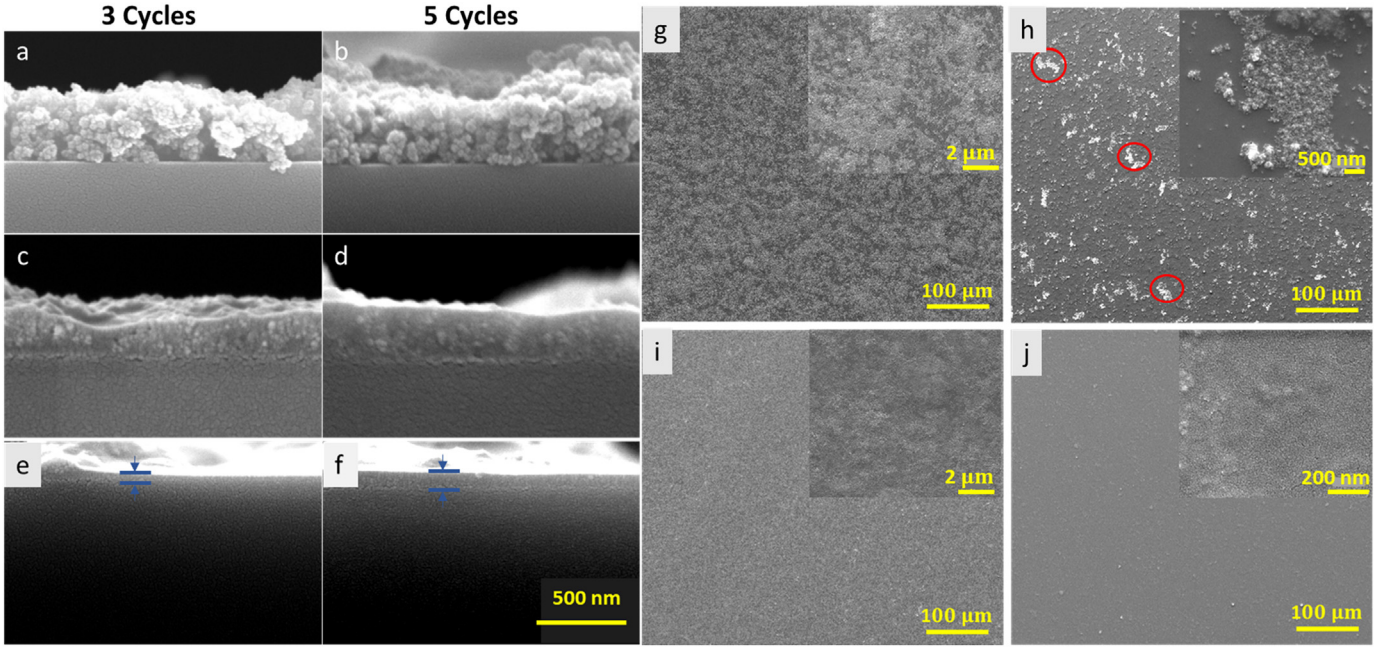

Fig. 4. Cross-sectional and top-view SEM images of the films created from ink A (a, b & g), ink B (h), ink C (c, d & i), and ink D (e, f & j). Three spin-coating cycles were applied in (a), (c) and (e), while five spin-coating cycles were used in (b), (d), (f) and (g) – (j). The red circles in (h) are examples of the YVO_4:Eu islands. A cross-sectional image of a discontinuous film made from ink B can be found in the supplementary material. The insets show high magnification images.

ten-cycle-coated sample. In comparison with the bare glass substrate, the graded thin film has a higher transmittance in the range of 400–675 nm and a slightly lower transmittance above 675 nm. We have to pointed out that the YVO_4:Eu-coated glass substrates have a transmittance peak that exceeds 100% in the UV range. This is due to the photoluminescence emission of YVO_4:Eu and the measuring apparatus (JASCO spectrophotometer). The photon detector used in the JASCO spectrophotometer was a photomultiplier tube (PMT) detector, which counted the number of incident photons but cannot distinguish the energy of photons. In our case, YVO_4:Eu absorbs UV photons and emits visible light, which means that when the UV light passed through the YVO_4:Eu-coated glass, both transmitted UV photons and emitted visible photons were counted as transmitted UV photons. As the PMT detector has a higher response to visible photons than UV photons, the presented transmittance can be higher than 100%. More substantial emission of YVO_4:Eu leads to a stronger transmittance signal in the UV region. The graded thin film has a transmittance peak as high as 120% (Fig. 5c), which is 30% and 10% higher than those of the bare glass substrate and the ten-cycle-coated sample, respectively. The graded thin film not only preserved the most transmittance in the visible region but also added YVO_4:Eu content, which enables more UV photons to be transformed into visible photons.

We placed the graded-thin-film-coated glass and bare glass substrates on top of the same pc-Si PV cell to measure the solar conversion efficiency. As shown in Table 3, the graded-thin-film-coated glass resulted in a higher short-circuit current density, JSC, and likewise a relative efficiency improvement of 4.12% compared to the uncoated cover glass. Fig. 5d shows that J_{SC} is elevated with coating of the graded thin film, which indicates an increased light-generated current, while the open-circuit voltage (V_{OC}) is maintained at 0.56 V. The maintained V_{OC} demonstrates unchanged carrier concentration and diffusion length of the solar cell. Fig. 5d clearly indicates that the SCE enhancement with the graded thin film is mainly attributed to the increased amount of available light and not to intrinsic variations of the solar cell. The enhanced SCE also can be witnessed in the external quantum efficiency tests between the samples with uncoated and graded-thin-film-coated glasses (supplementary material).

4. Conclusion

We designed, simulated, fabricated, and characterized graded thin films on the cover glass of pc-Si solar modules to harvest both UV and visible photons. The computational and experimental optical studies showed that a single layer of the downshifting phosphor YVO_4:Eu on a glass substrate resulted in a reduction of the transmittance in the visible region due to its unmatched refractive index with the glass substrate. HSNPs, which have a low RI of 1.12, were introduced into the YVO_4:Eu film to engineer the refractive index. The graded thin film of five layers with different RIs was applied to maintain the content of YVO_4:Eu required to capture UV photons without sacrificing the transmittance in the visible region. The RI and thickness of each layer of the graded thin film were deduced by the FDTD model, leading to an optimized transmittance in the range of 400–800 nm. The graded thin film that fabricated according to the FDTD model possessed a downshifting capability and increased the transmittance of visible photons. A 4.12% relative increment of the solar conversion efficiency of the pc-Si solar module was obtained by coating the graded thin film on the cover glass. The multifunctional thin films can harvest 31.8% of UV photons for solar electricity generation. To further improve the performance, the use of different downshifting materials to produce optimum spectra, tailored for solar cells, and the application of state-of-the-art upconverting nanophosphors [33] can be designed using our approach to achieve greater power enhancement. Since implementing multifunctional films on cover glass is well suited for the retrofit approach, the present solar technologies can utilize this technology without interfering with the manufacturing flow of solar modules.

CRediT authorship contribution statement

Yujuan He: Conceptualization, Methodology, Investigation, Software, Writing - original draft. **Jie Liu:** Software, Formal analysis. **Shi-Joon Sung:** Formal analysis, Validation. **Chih-hung Chang:** Conceptualization, Supervision, Writing - review & editing, Funding acquisition.

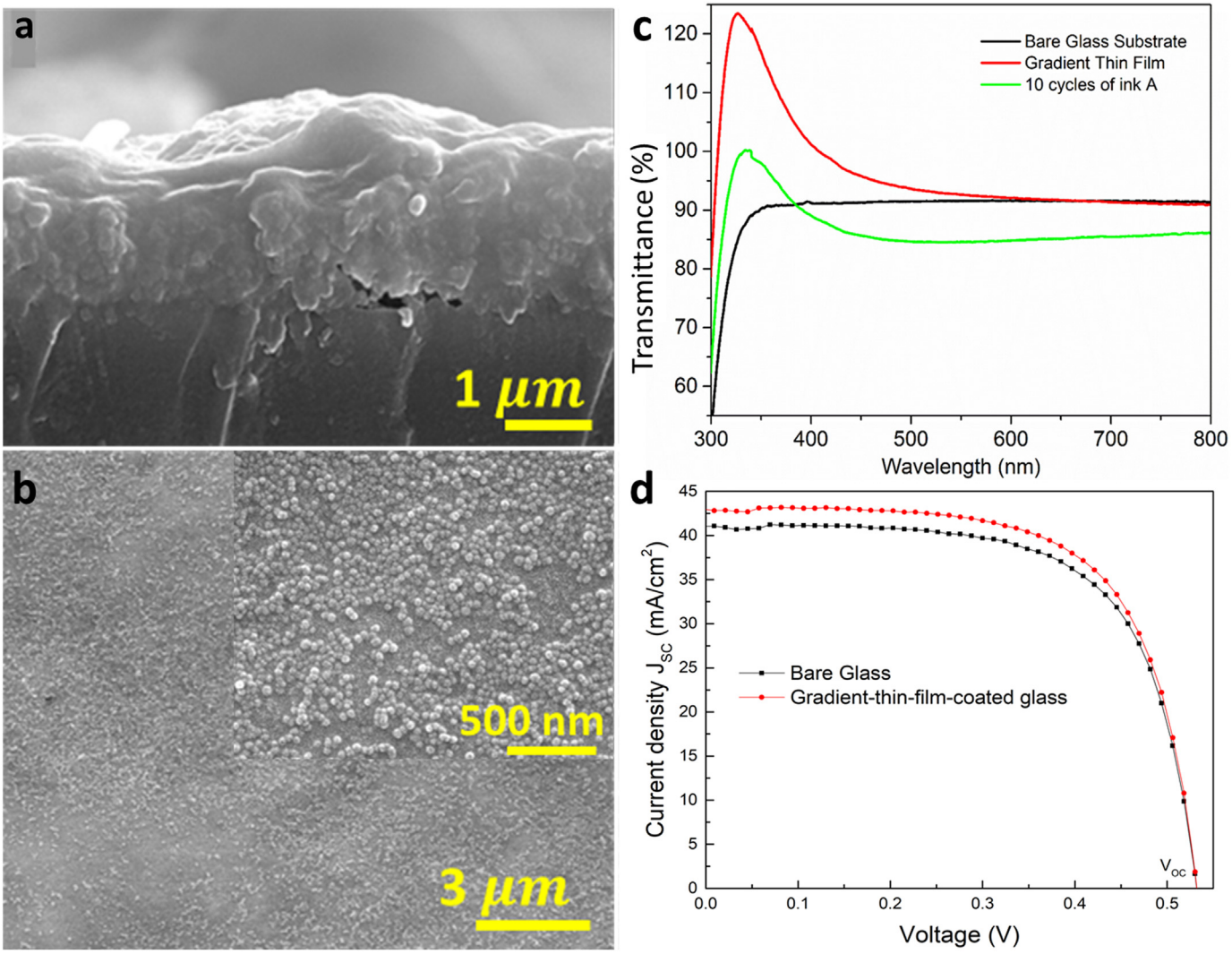

Fig. 5. (a) Cross-sectional and (b) top-view SEM images of the five-layer graded thin film with the optimized parameters. The red circles in (a) indicate the area of particles in the bulk film. (c) Transmittance spectra of the bare glass substrate, the ten-cycle-coated film of ink A and the graded thin film deposited on a glass substrate. (d) I-V curve of a pc-Si solar cell with graded thin film-coated and uncoated cover glass.

Table 3
SCE data of the pc-Si PV cells with the glass substrates placed on top.

	Open-circuit voltage (mV)	J_SC (mA cm^{-2})	Fill factor (%)	Efficiency (%)	[1]Relative improvement (%)
Bare Glass	528.34	41.04	66.37	14.39	–
Graded-thin-film-coated Glass	526.93	42.78	66.47	14.98	4.12%

[1] SCE improvement of the graded-thin-film-coated glass compared to the bare glass.

Declaration of Competing Interest

We wish to confirm that there are no known conflicts of interest associated with this publication and there has been no significant financial support for this work that could have influenced its outcome.

Acknowledgments

The NSF Scalable Nanomanufacturing program supports this work under Grant No. CBET-1449383. Part of this work was conducted at the Oregon Process Innovation Center, a National Nanotechnology Coordinated Infrastructure site at the Oregon State University, which is supported in part by the National Science Foundation (grant ECC-1542101) and Oregon State University. The TEM is funded by the National Science Foundation via the Major Research Instrumentation (MRI) Program under Grand No. 1040588. We thank Dr. Seung-Yeol Han for the technical editing that greatly improved the manuscript.

Appendix A. Supplementary data

Supplementary data to this article can be found online at https://doi.org/10.1016/j.matdes.2021.109454.

References

[1] G03 Committee, Tables for Reference Solar Spectral Irradiances: Direct Normal and Hemispherical on 37 degree Tilted Surface, Tech. rep, ASTM International, 2012https://doi.org/10.1520/G0173-03R12.

[2] Research Cell Efficiency Records. , Department of Energy, 2020https://www.energy.gov/eere/solar/downloads/research-cell-efficiency-records.
[3] H. Hovel, R. Hodgson, J. Woodall, The effect of fluorescent wavelength shifting on solar cell spectral response, Solar Energy Mater. 2 (1) (1979) 19–29, https://doi.org/10.1016/0165-1633(79)90027-3.
[4] E. Klampaftis, B.S. Richards, Improvement in multi-crystalline silicon solar cell efficiency via addition of luminescent material to EVA encapsulation layer, Prog. Photovolt. Res. Appl. 19 (3) (2011) 345–351, https://doi.org/10.1002/pip.1019.
[5] E. Klampaftis, D. Ross, S. Seyrling, A.N. Tiwari, B.S. Richards, Increase in short-wavelength response of encapsulated CIGS devices by doping the encapsulation layer with luminescent material, Sol. Energy Mater. Sol. Cells 101 (2012) 62–67, https://doi.org/10.1016/j.solmat.2012.02.011.
[6] L.D.A. Florêncio, L.A. Gómez-Malagón, B.C. Lima, A.S. Gomes, J. Garcia, L.R. Kassab, Efficiency enhancement in solar cells using photon down-conversion in Tb/Yb-doped tellurite glass, Sol. Energy Mater. Sol. Cells 157 (2016) 468–475, https://doi.org/10.1016/j.solmat.2016.07.024.
[7] S. Loos, F. Steudel, B. Ahrens, S. Schweizer, Optical properties of down-shifting barium borate glass for CdTe solar cells, Opt. Mater. 41 (2015) 143–145, https://doi.org/10.1016/j.optmat.2014.09.039.
[8] S. González-Pérez, J. Sanchiz, B. González-Díaz, S. Holinski, D. Borchert, C. Hernández-Rodríguez, R. Guerrero-Lemus, Luminescent polymeric film containing an Eu(III) complex acting as UV protector and down-converter for Si-based solar cells and modules, Surf. Coat. Technol. 271 (2015) 106–111, https://doi.org/10.1016/j.surfcoat.2014.12.074.
[9] G. Neuman, Anti-reflective coatings by APCVD using graded index layers, J. Non-Cryst. Solids 218 (1997) 92–99, https://doi.org/10.1016/S0022-3093(97)00160-9.
[10] Y.-Y. Lee, W.-J. Ho, C.-W. Yeh, Fabrication of silicon solar cell with >18% efficiency using spin-on-film processing for phosphorus diffusion and SiO2/graded index TiO2 anti-reflective coating, Appl. Surf. Sci. 354 (2015) 20–24, https://doi.org/10.1016/j.apsusc.2015.05.058.
[11] F.I. Chowdhury, A. Alnuaimi, N. El-Atab, M. Nayfeh, A. Nayfeh, Enhanced performance of thin-film amorphous silicon solar cells with a top film of 2.85 nm silicon nanoparticles, Sol. Energy 125 (2016) 332–338, https://doi.org/10.1016/j.solener.2015.12.030.
[12] X. Pi, Q. Li, D. Li, D. Yang, Spin-coating silicon-quantum-dot ink to improve solar cell efficiency, Sol. Energy Mater. Sol. Cells 95 (10) (2011) 2941–2945, https://doi.org/10.1016/j.solmat.2011.06.010.
[13] B.S. Richards, K.R. McIntosh, Overcoming the poor short wavelength spectral response of CdS/CdTe photovoltaic modules via luminescence down-shifting: ray-tracing simulations, Prog. Photovolt. Res. Appl. 15 (1) (2007) 27–34, https://doi.org/10.1002/pip.723.
[14] P. Chung, H.-h. Chung, P.H. Holloway, Phosphor coatings to enhance Si photovoltaic cell performance, J. Vac. Sci. Technol. A 25 (1) (2007) 61–66, https://doi.org/10.1116/1.2393298.
[15] J.-Y. Chen, C. Huang, W. Hung, K. Sun, T. Chen, Efficiency improvement of Si solar cells using metal-enhanced nanophosphor fluorescence, Sol. Energy Mater. Sol. Cells 120 (2014) 168–174, https://doi.org/10.1016/j.solmat.2013.08.039.
[16] X.Y. Huang, J.X. Wang, D.C. Yu, S. Ye, Q.Y. Zhang, X.W. Sun, Spectral conversion for solar cell efficiency enhancement using YVO4: Bi3+, Ln3+ (Ln = Dy, Er, Ho, Eu, Sm, and Yb) phosphors, J. Appl. Phys. 109 (11) (2011) 113526, https://doi.org/10.1063/1.3592889.
[17] B. Denker, E. Shklovsky, Handbook of Solid-State Lasers: Materials, Systems and Applications, Elsevier, 2013.
[18] R. Mohamed, F. Harraz, I. Mkhalid, Hydrothermal synthesis of size-controllable yttrium Orthovanadate (YVO4) nanoparticles and its application in photocatalytic degradation of direct blue dye, J. Alloys Compd. 532 (2012) 55–60, https://doi.org/10.1016/j.jallcom.2012.04.016.
[19] S. Chattopadhyay, Y. Huang, Y. Jen, A. Ganguly, K. Chen, L. Chen, Anti-reflecting and photonic nanostructures, Mater. Sci. Eng. R. Rep. 69 (1–3) (2010) 1–35, https://doi.org/10.1016/j.mser.2010.04.001.
[20] J. Jin, H. Li, C. Chen, B. Zhang, W. Bi, Z. Song, L. Xu, B. Dong, H. Song, Q. Dai, Improving efficiency and light stability of Perovskite solar cells by incorporating YVO4: Eu3+, Bi3+ Nanophosphor into the Mesoporous TiO2 layer, ACS Appl. Energy Mater. 1 (5) (2018) 2096–2102, https://doi.org/10.1021/acsaem.8b00192.
[21] C. Huang, Y. Chen, W. Hung, T. Chen, K. Sun, W. Chang, Enhanced light harvesting of Si solar cells via luminescent down-shifting using YVO4: Bi3+, Eu3+ nanophosphors: enhanced light harvesting of Si solar cells using YVO4 nanophosphors, Prog. Photovolt. Res. Appl. 21 (7) (2013) 1507–1513, https://doi.org/10.1002/pip.2222.
[22] N. Chander, S.K. Sardana, P.K. Parashar, A.F. Khan, S. Chawla, V.K. Komarala, Improving the short-wavelength spectral response of silicon solar cells by spray deposition of YVO4: Eu3+ downshifting phosphor nanoparticles, IEEE J. Photovolt. 5 (5) (2015) 1373–1379, https://doi.org/10.1109/JPHOTOV.2015.2438633.
[23] Y. He, K.-J. Kim, C.-H. Chang, Continuous, size and shape-control synthesis of hollow silica nanoparticles enabled by a microreactor-assisted rapid mixing process, Nanotechnology 28 (23) (2017) 235602, https://doi.org/10.1088/1361-6528/aa6fa7.
[24] A. Huignard, T. Gacoin, J.-P. Boilot, Synthesis and luminescence properties of colloidal YVO4: Eu phosphors, Chem. Mater. 12 (4) (2000) 1090–1094.
[25] E. Klampaftis, D. Ross, K.R. McIntosh, B.S. Richards, Enhancing the performance of solar cells via luminescent down-shifting of the incident spectrum: a review, Sol. Energy Mater. Sol. Cells 93 (8) (2009) 1182–1194, https://doi.org/10.1016/j.solmat.2009.02.020.
[26] Average Solar Panel Dimensions and Sizes, URL https://news.energysage.com/average-solar-panel-size-weight/ Oct 2016.
[27] 2018 Average Solar Panel Size and Weight. , EnergySage, Jan 2018https://news.energysage.com/average-solar-panel-size-weight/.
[28] R. Fu, D. Feldman, R. Margolis, M. Woodhouse, K. Ardani, U.S. Solar Photovoltaic System Cost Benchmark: Q1 2017, Renew. Energy (2017) 73.
[29] Refractive Index of BK7 - SCHOTT, URL https://refractiveindex.info/?shelf=glass&book=BK7&page=SCHOTT 2020.
[30] T. Jia, Y. Zhang, J. Chen, Simulation of granular packing of particles with different size distributions, Comput. Mater. Sci. 51 (1) (2012) 172–180, https://doi.org/10.1016/j.commatsci.2011.07.044.
[31] P. Buskens, M. Burghoorn, M.C.D. Mourad, Z. Vroon, Antireflective coatings for glass and transparent polymers, Langmuir 32 (27) (2016) 6781–6793, https://doi.org/10.1021/acs.langmuir.6b00428.
[32] M. Keshavarz Hedayati, M. Elbahri, Antireflective coatings: conventional stacking layers and ultrathin Plasmonic Metasurfaces, a mini-review, Materials 9 (6) (2016) 497, https://doi.org/10.3390/ma9060497.
[33] Y. Sun, X. An, L. Chen, Q. Gao, X. Zhang, L. Duan, W. Lü, Upconverting nanophosphor incorporated photoanodes for improved photoelectric performances of quantum dot sensitized solar cells, Mater. Res. Lett. 6 (6) (2018) 314–320, https://doi.org/10.1080/21663831.2018.1447521.